arXiv:nucl-th/9212008 v1 15 Dec 1992

MIT-CTP-2169 / ORNL-CCIP-92-15

Kaon-Nucleon Scattering Amplitudes and Z*-Enhancements from Quark Born Diagrams

T.Barnes
Physics Division and Center for Computationally Intensive Physics
Oak Ridge National Laboratory, Oak Ridge, TN 37831-6373
and
Department of Physics
University of Tennessee, Knoxville, TN 37996-1200

E.S.Swanson
Center for Theoretical Physics
Laboratory of Nuclear Science and Department of Physics
Massachusetts Institute of Technology, Cambridge, MA 02139

We derive closed form kaon-nucleon scattering amplitudes using the "quark Born diagram" formalism, which describes the scattering as a single interaction (here the OGE spin-spin term) followed by quark line rearrangement. The low energy I=0 and I=1 S-wave KN phase shifts are in reasonably good agreement with experiment given conventional quark model parameters. For $k_{lab} > 0.7$ Gev however the I=1 elastic phase shift is larger than predicted by Gaussian wavefunctions, and we suggest possible reasons for this discrepancy. Equivalent low energy KN potentials for S-wave scattering are also derived. Finally we consider OGE forces in the related channels KΔ, K*N and K*Δ, and determine which have attractive interactions and might therefore exhibit strong threshold enhancements or "Z*-molecule" meson-baryon bound states. We find that the minimum-spin, minimum-isospin channels and two additional K*Δ channels are most conducive to the formation of bound states. Related interesting topics for future experimental and theoretical studies of KN interactions are also discussed.

December 1992

I. INTRODUCTION

Kaon-nucleon collisions allow one to address many interesting problems in nuclear and hadron physics [1]. (By "kaons" we refer to the $K^+ = u\bar{s}$ and $K^0 = d\bar{s}$, generically K, as distinct from the $\bar{K}$ antikaons $K^- = s\bar{u}$ and $\bar{K}^0 = s\bar{d}$.) Three familiar examples which we shall discuss below are 1) the origins of nonresonant "nuclear" forces in a system distinct from NN, 2) nuclear structure physics, using kaons as weakly scattered probes, and 3) searches for possible exotic Z^* baryon resonances which couple directly to KN. More recently it has become clear that an understanding of KN scattering in nuclear matter is important in other areas, such as the interpretation of strangeness production in nuclear collisions and in two-kaon correlation measurements [2].

Elastic KN scattering is a natural system for the study of nonresonant nuclear forces. Since the valence kaon wavefunction contains an $\bar{s}$ antiquark which cannot annihilate against the nonstrange nucleon state, direct production of conventional baryon resonances is excluded. KN scattering is further simplified by the absence of one pion exchange, so one can study the nonresonant, non-OPE part of hadron scattering in relative isolation. Theoretical studies of KN nuclear forces are especially appropriate because there is already considerable experimental information on the elastic amplitudes and two-body inelastic reactions such as KN$\rightarrow$ K*N and KN$\rightarrow$ KΔ [1,3–5]. These experimental amplitudes provide stringent tests for models of hadronic interactions. The dominant S-wave elastic phase shifts are moderately well established, and the higher partial waves up to L=4 have been determined or estimated [5]. The basic features of the elastic reaction are a strong repulsion in the I=1 S-wave, a weaker repulsion in the I=0 S-wave, and an important spin-orbit interaction which is evident in the P-waves. The important low energy behavior of the I=0 S-wave, in particular the scattering length, is unfortunately not yet very well known. The experimental situation should improve considerably with the development of new hadronic facilities such as DAΦNE and KAON [6,7].

KN scattering also has applications in nuclear physics; since the kaon-nucleon cross section is relatively small, kaon beams can be used as probes of nuclear structure. It would obviously be useful to understand the mechanism and properties of the kaon-nucleon interaction for this application. In view of this application one topic in this paper will be the derivation of effective low energy KN potentials from the nonrelativistic quark potential model.

Another reason for interest in KN collisions is the possibility of producing flavor-exotic Z^* baryon resonances. If discovered, these might be resonances with the quark valence structure $q^4\bar{s}$ [8], where $q = u$ or d. Such multiquark hadrons were widely predicted in the early days of the quark model [9], but it now appears that multiquark basis states usually do not support resonances, due to the "fall apart" effect [10,11]. The known exceptions are deuteronlike "molecule" states of hadron pairs, which should perhaps be classified as unusual nuclear species. (Nuclei themselves are excellent examples of the tendency of multiquark systems to separate into hadronic molecules.) In the meson-meson sector two $K\bar{K}$ molecule states are reasonably well established [12], and there are several other meson-meson candidates [13]. In the antikaon-nucleon sector the $\Lambda(1405)$ is an obvious candidate $\bar{K}$N molecule, and there presumably are other molecule states in channels with attractive interactions. Both the elastic reaction KN$\rightarrow$KN and inelastic processes such as KN$\rightarrow$ K*N and KN$\rightarrow$ KΔ can be studied for evidence of exotic Z* baryon resonances. With a realistic model of hadronic interactions we might reasonably expect to predict the quantum numbers of exotic meson-baryon molecular bound states, should these exist.

In this paper we apply the "quark Born diagram" formalism to KN scattering. In this approach we assume conventional nonrelativistic quark model wavefunctions for the asymptotic hadrons, and calculate the Hamiltonian matrix element for scattering due to a single interaction between constituents in different incident hadrons. To form color singlet final states at lowest order one must then exchange constituents. The full Born amplitude is obtained by summing over all such processes coherently. (Similar constituent exchange mechanisms have been proposed for high energy hadron scattering [14], and there is strong experimental evidence in favor of this mechanism from large-t exclusive reactions [15].) This nonrelativistic Hamiltonian matrix element is then combined with relativistic phase space and kinematics to give results for differential cross sections, partial wave amplitudes and other scattering observables. In previous work we derived the elastic scattering amplitudes for I=2 $\pi\pi$ [16], I=3/2 Kπ [17] and I=1 KK [16]. (These cases were chosen because they are free of valence $q\bar{q}$ annihilation processes, which are known to be important if allowed.) We found good agreement with experimental $\pi\pi$ and Kπ S-wave phase shifts given conventional quark model parameters. We have also applied similar techniques to pseudoscalar-vector and vector-vector meson channels [18], and the results may have important implications for meson spectroscopy [13]. In Appendix C of [16] we presented a diagrammatic representation of these techniques, with associated "Feynman rules" for the scattering diagrams. KN elastic scattering is also annihilation free and affords a nontrivial test of the quark Born formalism.

KN elastic scattering has previously been the subject of numerous theoretical investigations. Meson exchange models have been applied in several studies [19], but these are difficult to justify fundamentally because the range of heavier meson exchange forces (≈ 0.2 fm) is much smaller than the minimum possible interhadron distance for two distinct hadrons (≈ 1 fm) [11]. These models typically have many free parameters, which are not well established experimentally and are fitted to the data. Thus one is in effect simply parametrizing experiment. This type of model may be of theoretical interest as a parametrization of more fundamental scattering mechanisms which operate at the quark and gluon level, as it may be possible to relate the predictions of these different approaches.

A quark and gluon approach to scattering using the P-matrix and bag model wavefunctions was proposed by Jaffe and Low [20]. They suggested interpreting the multiquark clusters of the bag model not as resonances, but instead as the short distance parts of hadron-hadron scattering states. In principal this approach can be used to predict phase shifts, but in practice it has mainly been used to interpret experimental phase shifts in terms of P-matrix poles. This approach has been followed for KN by Roiesnal [21], who concluded that the KN data could indeed be interpreted in terms of poles approximately at the energies predicted by the bag model, but that the pole residues (coupling strengths to asymptotic KN channels) did not agree well with predictions. A more recent bag model calculation of KN scattering by Veit, Thomas and Jennings [22] used the cloudy bag model, which combines quark fields (in the baryon) with fundamental pseudoscalar meson fields in an effective lagrangian. This composite model leads to an I=1 S-wave phase shift and a scattering length which are very similar to our result, but their I=0 phase shift is much smaller than experiment. Although this cloudy bag approach gives promising numerical results, it does not provide us with an understanding of the scattering mechanism at the quark and gluon level.

Studies of the dominant S-wave KN scattering amplitudes in terms of quark model wavefunctions and quark-gluon interactions have been published by Bender and Dosch [23] (adiabatic approach), Bender, Dosch, Pirner and Kruse [24] (variational generator coordinate method, GCM) and Campbell and Robson [25] (resonating group method, RGM). The large spin-orbit forces evident in the KN P-wave data have also been studied using similar quark model techniques, first qualitatively by Pirner and Povh [26] and later in detail by Mukhopadhyay and Pirner [27] (using GCM). The assumptions regarding dynamics, the scattering mechanism, quark model wavefunctions and the parameters used in these calculations are very similar to our assumptions in this paper. The most important differences are that 1) our techniques are perturbative and allow analytic solution, and 2) we disagree about the size of the OGE contribution to KN scattering. Specifically, we find that OGE alone suffices to explain the observed I=1 KN scattering length, whereas Bender *et al.* [24] conclude that OGE is too small, and that a Pauli blocking effect is dominant in I=1. Campbell and Robson [25] similarly found that the experimental I=1 phase shift was larger than their predictions, which were based on generalizations of Gaussian wavefunctions and a full OGE and confining interaction.

II. CALCULATION OF KN AND RELATED SCATTERING AMPLITUDES

a) Hamiltonian and hadron states

Our technique involves a Born order calculation of the matrix element of the Hamiltonian between asymptotic hadron states in the nonrelativistic quark model. In the KN case the dominant interaction was previously found by Bender *et al.* [24] to be the spin-spin "color hyperfine" term. A similar conclusion has been reached for the NN interaction [11,28]. Here we shall adopt this approximation and neglect the other OGE and confining terms. Thus, our scattering amplitude is proportional to the matrix element of

$$H_{scat} = \sum_{a,i<j} \left[-\frac{8\pi\alpha_s}{3m_i m_j}\, \delta(\vec{r}_{ij}) \right] \left[\vec{S}_i \cdot \vec{S}_j \right] \left[\mathcal{F}^a_i \cdot \mathcal{F}^a_j \right] \tag{1}$$

between asymptotic KN states. ($\mathcal{F}^a_i$ is the color matrix for quark or antiquark i, which is $\lambda^a/2$ for quarks and $-(\lambda^T)^a/2$ for antiquarks.) Although we shall quote results for arbitrary asymptotic hadron wavefunctions, we shall specialize to Gaussian wavefunctions for our numerical results, as these allow closed form derivation of scattering observables. Our momentum space Gaussian wavefunctions for the kaon and nucleon are conventional quark model forms,

$$\phi_{kaon}(\vec{p}_{rel}) = \frac{1}{\pi^{3/4}\beta^{3/2}} \exp\left\{ -\frac{\vec{p}^{\,2}_{rel}}{8\beta^2} \right\} \tag{2}$$

where

$$\vec{p}_{rel} \equiv \frac{(m_{\bar q}\vec{p}_q - m_q\vec{p}_{\bar q})}{(m_q + m_{\bar q})/2} \;, \tag{3}$$

and

$$\phi_{nucleon}(\vec{p}_1,\vec{p}_2,\vec{p}_3) = \frac{3^{3/4}}{\pi^{3/2}\alpha^3}\exp\Big\{ -\frac{(\vec{p}_1^{\,2}+\vec{p}_2^{\,2}+\vec{p}_3^{\,2}-\vec{p}_1\cdot\vec{p}_2-\vec{p}_2\cdot\vec{p}_3-\vec{p}_3\cdot\vec{p}_1)}{3\alpha^2}\Big\} \ . \tag{4}$$

The parameters α and β are typically found to be $\approx 0.3-0.4$ Gev in hadron phenomenology. These are relative momentum wavefunctions, and have an implicit constraint that the constituent momenta add to the hadron momentum. In the full momentum space wavefunction there is an overall delta function that imposes this constraint;

$$\Phi_{kaon}(\vec{p}_q,\vec{p}_{\bar q};\vec{P}_{tot}) = \phi_{kaon}(\vec{p}_{rel})\ \delta(\vec{P}_{tot}-\vec{p}_q-\vec{p}_{\bar q}) \ , \tag{5}$$

$$\Phi_{nucleon}(\vec{p}_1,\vec{p}_2,\vec{p}_3;\vec{P}_{tot}) = \phi_{nucleon}(\vec{p}_1,\vec{p}_2,\vec{p}_3)\ \delta(\vec{P}_{tot}-\vec{p}_1-\vec{p}_2-\vec{p}_3) \ . \tag{6}$$

The normalizations are

$$\langle\Phi_{kaon}(\vec{P}'_{tot})|\Phi_{kaon}(\vec{P}_{tot})\rangle$$

$$= \iiiint d\vec{p}\,d\vec{\bar p}\,d\vec{p}\,'\,d\vec{\bar p}\,'\,\Phi^*_{kaon}(\vec{p}\,',\vec{\bar p}\,';\vec{P}'_{tot})\Phi_{kaon}(\vec{p},\vec{\bar p};\vec{P}_{tot}) = \delta(\vec{P}_{tot}-\vec{P}'_{tot}) \tag{7}$$

and

$$\langle\Phi_{nucleon}(\vec{P}'_{tot})|\Phi_{nucleon}(\vec{P}_{tot})\rangle$$

$$= \int\!\!\int\!\!\int\!\!\int\!\!\int\!\!\int d\vec{p}_1\,d\vec{p}_2\,d\vec{p}_3\,d\vec{p}_1\,'\,\vec{p}_2\,'\,d\vec{p}_3\,'\,\Phi^*_{nucleon}(\vec{p}_1\,',\vec{p}_2\,',\vec{p}_3\,';\vec{P}'_{tot})\Phi_{nucleon}(\vec{p}_1,\vec{p}_2,\vec{p}_3;\vec{P}_{tot})$$

$$= \delta(\vec{P}_{tot}-\vec{P}'_{tot}) \ . \tag{8}$$

Since these state normalizations are identical to those used in our previous study of Kπ scattering [17] we can use the relations between amplitudes and scattering observables given in that reference.

The color wavefunctions for the asymptotic hadrons are the familiar color singlet states

$$|meson\rangle = \sum_{\imath,\bar\imath=1,3}\frac{1}{\sqrt{3}}\,\delta_{\imath\bar\imath}\ |\imath\bar\imath\rangle \tag{9}$$

and

$$|baryon\rangle = \sum_{i,j,k=1,3}\frac{1}{\sqrt{6}}\,\epsilon_{ijk}\ |ijk\rangle \ . \tag{10}$$

Our spin-flavor states for the meson and baryon are standard SU(6) states, but we have found it convenient to write the baryon states in an unconventional manner, as the usual quark model conventions are unwieldy for our purposes. First, to establish our notation, the spin-flavor K$^+$ state is

$$|\mathrm{K}^+\rangle = \frac{1}{\sqrt{2}}\Big(|u_+\bar{s}_-\rangle - |u_-\bar{s}_+\rangle \Big) \ . \tag{11}$$

For quark model baryon states it is conventional to assign each quark a fixed location in the state vector, as though identical quarks were distinguishable fermions. One then explicitly symmetrizes this state. Thus for example one writes the normalized $\Delta^+(S_z = +3/2)$ state as

$$|\Delta^+(+3/2)\rangle = \frac{1}{\sqrt{3}}\Big(|u_+u_+d_+\rangle + |u_+d_+u_+\rangle + |d_+u_+u_+\rangle \Big) \tag{12}$$

and treats each basis state as orthogonal. Note however that this is not the usual way to represent multifermion states. In standard field theoretic usage each of these basis states is identical to the others, to within an overall phase. In this language the normalized $\Delta^+(+3/2)$ state is simply

$$|\Delta^+(+3/2)\rangle = \frac{1}{\sqrt{2}} \ |u_+u_+d_+\rangle \ , \tag{13}$$

which we could equally well write as $|u_+d_+u_+\rangle/\sqrt{2}$ or $|d_+u_+u_+\rangle/\sqrt{2}$. The advantage of using field theory conventions becomes clear in calculating nucleon matrix elements. For example, the usual quark model proton state is

$$\begin{aligned} |P(+1/2)\rangle = \ & \Big(\ 2|u_+u_+d_-\rangle - |u_+u_-d_+\rangle - |u_-u_+d_+\rangle \\ & + 2|u_+d_-u_+\rangle - |u_+d_+u_-\rangle - |u_-d_+u_+\rangle \\ & + 2|d_-u_+u_+\rangle - |d_+u_+u_-\rangle - |d_+u_-u_+\rangle \Big) \Big/ \sqrt{18} \ , \end{aligned} \tag{14}$$

and in comparison this state in field theory conventions is

$$|P(+1/2)\rangle = \sqrt{\frac{2}{3}} \ \left\{ \frac{|u_+u_+d_-\rangle}{\sqrt{2}} \right\} - \sqrt{\frac{1}{3}} \ |u_+u_-d_+\rangle \ . \tag{15}$$

Use of the latter form, with all permutations of quark entries allowed in matrix elements, reduces the number of P→P terms from 81 (many of which are zero) to 4. Of course the results are identical, as these are just different conventions for the same state.

b) Enumeration of quark line diagrams for KN

Now we consider KN scattering. As explained in reference [16], we begin by determining the matrix element of the scattering Hamiltonian (1). First we factor out the overall momentum conserving delta function and then derive the remaining matrix element, which we call h_{fi};

$${}_f\langle KN|H_{scat}|KN\rangle_i \equiv h_{fi} \ \delta(\vec{P}_f - \vec{P}_i) \ . \tag{16}$$

We will discuss one part of the calculation in detail to explain the techniques, and then simply quote the full result. Specializing to the spin up I=1 case $\mathrm{K}^+\mathrm{P}(+1/2)\to\mathrm{K}^+\mathrm{P}(+1/2)$, we require the matrix element of the scattering hamiltonian (1) between initial and final $\mathrm{K}^+\mathrm{P}$

states with color and spin-flavor wavefunctions given by (9,10) and (11,15) respectively. Since the kaon and proton states (11) and (15) are each the sum of two terms, the full amplitude for $K^+P(+1/2) \to K^+P(+1/2)$ is a weighted sum of 16 subamplitudes. We shall consider the subamplitude for $|u_+\bar{s}_-\rangle\{|u_+u_+d_-\rangle/\sqrt{2}\} \to |u_+\bar{s}_-\rangle|u_+u_-d_+\rangle$, which we call $h^{e.g.}_{fi}$, in detail for illustration.

We begin by constructing all allowed quark line diagrams and their associated combinatoric factors. First we arrange the initial and final states with their normalizations on a generic scattering diagram,

$h^{e.g.}_{fi} \quad =$ 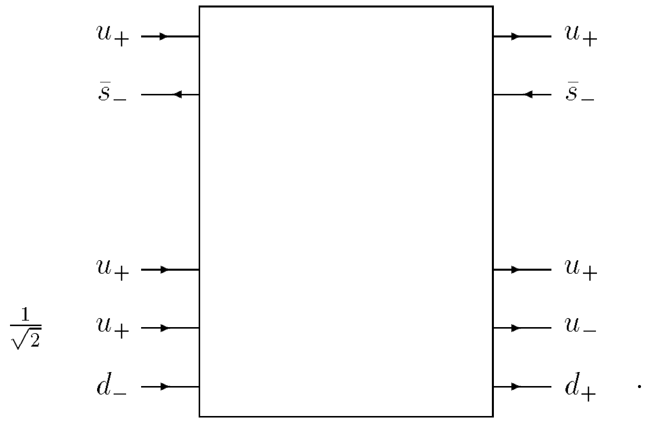 (17)

Now we connect the initial and final lines in all possible ways consistent with flavor conservation. For the d quark and the $\bar{s}$ antiquark this choice is unique. For the final meson's u quark however there are two choices for which initial baryon's quark it originates from. Similarly the initial meson's u quark can attach to either of two final baryon u quarks. Thus we have four quark line diagrams. We may immediately simplify the diagrams; since the baryon wavefunctions are symmetric, we may permute any two initial or final baryon lines and obtain an equivalent diagram. We use this symmetry to reduce all diagrams to a "standard form" in which only the meson's quark and the upper baryon quark are exchanged. The two choices for the initial baryon's spin up u_+ quark are thus equivalent, and contribute an overall combinatoric factor of two. The final baryon's quarks however give inequivalent diagrams, one being nonflip ($u_+(K) \to u_+(P)$) and the other spin flip ($u_+(K) \to u_-(P)$). (No polarization selection rules are being imposed yet, only flavor conservation.) Thus our amplitude leads to the line diagrams

$h^{e.g.}_{fi} = \frac{1}{\sqrt{2}} \cdot 2 \cdot$ 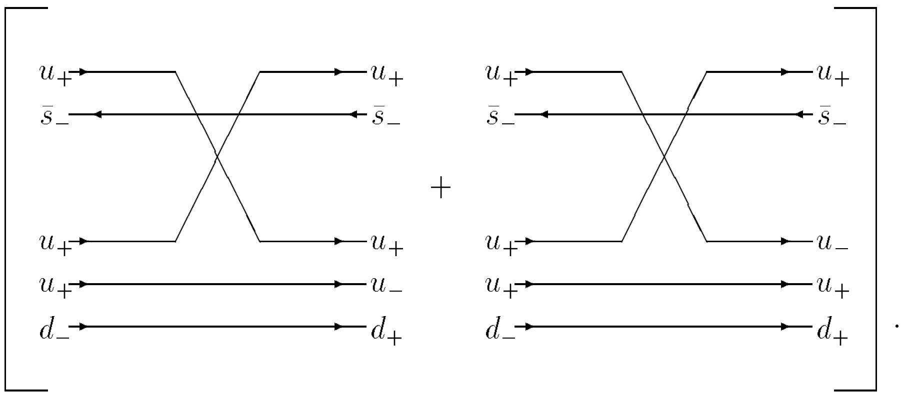 (18)

We next "decorate" each of these line diagrams with all possible single interactions (1) between a quark (or antiquark) in the initial meson and a quark in the initial baryon. There are six of these per line diagram (two choices in the meson times three in the baryon), so we have a total of twelve scattering diagrams to evaluate. However in this case all but one are trivially zero. Note that in the first line diagram we must flip the spins of u and d quarks in the initial baryon to have a nonzero contribution. This however is not part of our scattering interaction, which operates between pairs of constituents in different initial hadrons. The $\vec{S}_i \cdot \vec{S}_j$ interaction either flips a pair of spins in different incident hadrons (through S_+S_- or S_-S_+ terms) or leaves all spins unchanged (through S_zS_z). Thus, the transition in the first line diagram cannot occur through a single $\vec{S}_i \cdot \vec{S}_j$ interaction. For the second diagram however there is a single nonvanishing transition, in which the initial meson's u_+ quark and the baryon's d_- quark interact through the spin flip operator;

$$h_{fi}^{e.g.} \quad = \quad \sqrt{2} \quad \cdot \tag{19}$$

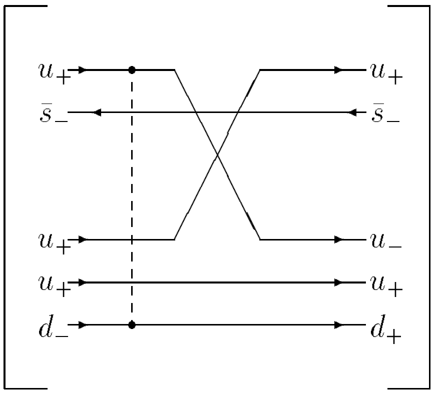

.

c) Independent quark and gluon diagrams and their spin and color factors

Finally we require the spin, color, overall phase and spatial factors associated with this and the other independent diagrams. There are only four independent quark and gluon diagrams, since all others can be obtained from these by permutation of lines. These four diagrams are

$$D_1 \quad = \tag{20}$$

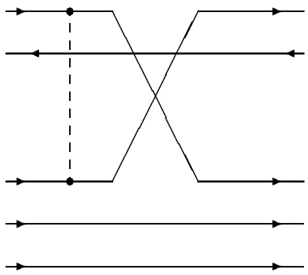

,

$D_2 =$ 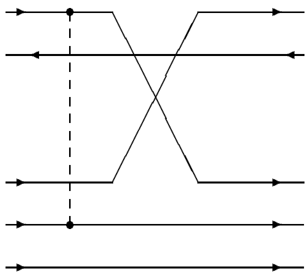 , (21)

$D_3 =$ 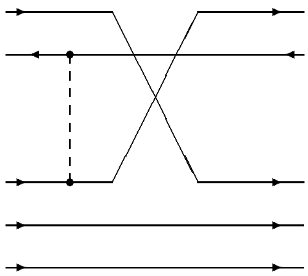 , (22)

$D_4 =$ 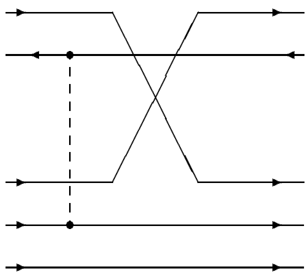 . (23)

The spin factor is simply the matrix element of $\vec{S}_i \cdot \vec{S}_j$ for scattering constituents i and j, evaluated between the initial and final $(q\bar{q})(qqq)$ spin states. This is $1/2$ if both spins i and j are antialigned and both flip, $+1/4$ if the spins are aligned and neither flips, and $-1/4$ if they are antialigned and neither flips. All other cases give zero. All spectator spins must not flip or the overall spin factor is trivially zero.

The color factor can be evaluated using the states (9), (10) and standard trace techniques, as in (51) of reference [16]. The result for each diagram is

$$I_{\rm color}(D_1) = +4/9 \ , \tag{24}$$

$$I_{\rm color}(D_2) = -2/9 \ , \tag{25}$$

$$I_{\rm color}(D_3) = -4/9 \ , \tag{26}$$

$$I_{\rm color}(D_4) = +2/9 \ . \tag{27}$$

d) "Diagram weights" for KN scattering

We conventionally write the meson-baryon h_{fi} matrix elements as row vectors which display the numerical coefficient of each diagram's spatial overlap integral. Thus,

$$h_{fi} = \Big[\ w_1,\ w_2,\ w_3,\ w_4\ \Big] \tag{28}$$

represents

$$h_{fi} = w_1\, I_{\rm space}(D_1)\ + w_2\, I_{\rm space}(D_2)\ + w_3\, I_{\rm space}(D_3)\ + w_4\, I_{\rm space}(D_4)\ . \tag{29}$$

This notation is useful because the diagram weights $\{w_i\}$ are group theoretic numbers that obey certain symmetries, whereas the spatial overlap integrals are complicated functions that depend on the specific spatial wavefunctions rather than the symmetries of the problem.

As an illustration, our practice subamplitude $h_{fi}^{e.g.}$ is

$$h_{fi}^{e.g.} = \sqrt{2}\cdot\Big(\frac{1}{2}\Big)\cdot\Big(-\frac{2}{9}\Big)\cdot I_{\rm space}(D_2)\ . \tag{30}$$

(using the spin and color matrix elements given above), which we abbreviate as

$$h_{fi}^{e.g.} = \Big[\ 0,\ -\frac{\sqrt{2}}{9},\ 0,\ 0\ \Big]\ . \tag{31}$$

This completes our detailed derivation of $h_{fi}^{e.g.}$ for the subprocess $|u_+\bar s_-\rangle\{|u_+u_+d_-\rangle/\sqrt{2}\}\to |u_+\bar s_-\rangle|u_+u_-d_+\rangle$.

Proceeding similarly, we have derived the weights for the full KN elastic scattering amplitudes, given the states (11) and (15) and their isospin partners. These are

$$h_{fi}^{\rm KN}({\rm I}=0) = \Big[\ 0,\ \frac{1}{6},\ 0,\ \frac{1}{6}\ \Big] \tag{32}$$

and

$$h_{fi}^{\rm KN}({\rm I}=1) = \Big[\ \frac{1}{3},\ \frac{1}{18},\ \frac{1}{3},\ \frac{1}{18}\ \Big]\ . \tag{33}$$

For numerical estimates of these amplitudes we require the spatial overlap integrals, which we shall evaluate explicitly with Gaussian wavefunctions.

e) Spatial overlap integrals

The spatial overlap integrals represented by the four diagrams $D_1 \ldots D_4$ may be determined using the diagrammatic techniques discussed in Appendix C of reference [16]. These are formally 30-dimensional overlap integrals (three dimensions times ten external lines), but twelve integrations are eliminated by external momentum constraints and an additional nine are eliminated by the unscattered spectator lines. This leaves a nontrivial 9-dimensional overlap integral for each diagram. We give the initial meson a label A, with three-momentum also called A and quark three-momentum a and antiquark momentum $\bar a$, and we similarly label the initial baryon B, the final meson C and the final baryon D. Since we choose to evaluate these integrals in the CM frame we use the momentum substitutions $B=-A$ and

$D = -C$. We also introduce a nonstrange to strange quark mass ratio $\rho = m_q/m_s$. With these substitutions the four spatial overlap integrals are

$$I_{space}(D_1) = +\frac{8\pi\alpha_s}{3m_q^2}\,\frac{1}{(2\pi)^3}\iiint d\vec{a}\,d\vec{b}_1\,d\vec{b}_2\;\phi_A(2a - \frac{2\rho A}{1+\rho})\;\phi_C^*(2a + \frac{2C}{1+\rho} - 2A)$$

$$\cdot\;\phi_B(b_1, b_2, -A - b_1 - b_2)\;\phi_D^*(b_1 + A - C, b_2, -A - b_1 - b_2)\;, \tag{34}$$

$$I_{space}(D_2) = +\frac{8\pi\alpha_s}{3m_q^2}\,\frac{1}{(2\pi)^3}\iiint d\vec{b}_1\,d\vec{c}\,d\vec{d}_1\;\phi_A(2c - \frac{2A}{1+\rho} - 2C)\;\phi_C^*(2c - \frac{2\rho C}{1+\rho})$$

$$\cdot\;\phi_B(b_1, c, -A - b_1 - c)\;\phi_D^*(d_1, A - C + b_1 + c - d_1, -A - b_1 - c)\;, \tag{35}$$

$$I_{space}(D_3) = +\frac{8\pi\alpha_s}{3m_q^2}\rho\,\frac{1}{(2\pi)^3}\iiint d\vec{a}\,d\vec{b}_2\,d\vec{c}\;\phi_A(2a - \frac{2\rho A}{1+\rho})\;\phi_C^*(2c - \frac{2\rho C}{1+\rho})$$

$$\cdot\;\phi_B(a - A + C, b_2, -a - b_2 - C)\;\phi_D^*(a, b_2, -a - b_2 - C)\;, \tag{36}$$

$$I_{space}(D_4) = +\frac{8\pi\alpha_s}{3m_q^2}\rho\,\frac{1}{(2\pi)^3}\iiint d\vec{a}\,d\vec{b}_1\,d\vec{c}\;\phi_A(2a - \frac{2\rho A}{1+\rho})\;\phi_C^*(2c - \frac{2\rho C}{1+\rho})$$

$$\cdot\;\phi_B(b_1, c, -A - b_1 - c)\;\phi_D^*(A - C - a + b_1 + c, a, -A - b_1 - c)\;. \tag{37}$$

There are many equivalent ways to write these integrals which arise from different choices of the variables eliminated by momentum constraints.

Note that the overall coefficients of these integrals are positive, although the coefficient of H_{scat} (1) is negative. This is because there is an overall phase factor of (-1) for each diagram $D_1 \ldots D_4$, due to anticommutation of quark creation and annihilation operators in the matrix element. Here we incorporate this phase, which we call the "signature" of the diagram [16], in the spatial overlap integrals. The signature is equal to $(-1)^{N_x}$, where N_x is the number of fermion line crossings. For diagrams $D_1 \ldots D_4$ above $N_x = 3$, so the signature is

$$I_{\text{signature}} = (-1)\;. \tag{38}$$

Note that a diagram in nonstandard form, such as the kaon's quark line crossing to the second baryon quark, can have a $(+1)$ signature; in the full h_{fi} matrix element this is compensated by a change in sign of the color factor.

We explicitly evaluate these overlap integrals using the Gaussian wavefunctions (2) and (4). For Gaussians the integrals factor into products of three 3-dimensional integrals, and the results are all of the form

$$I_{\text{space}}(D_i) = \frac{8\pi\alpha_s}{3m_q^2}\frac{1}{(2\pi)^3}\;\eta_i \exp\Big\{ - (A_i - B_i\mu)P_{cm}^2 \Big\}\;, \tag{39}$$

where P_{cm}^2 is the modulus of each hadron's three-momentum in the CM frame, $\mu = \cos(\theta_{CM})$ where θ_{CM} is the CM scattering angle, and the constants η_i, A_i and B_i are functions of α, β and ρ. $B_i > 0$ implies forward peaked scattering and $B_i < 0$ is backward peaking. The pure exponential dependence in P_{cm}^2 and $P_{cm}^2\mu$ is a consequence of the Gaussian wavefunctions and the contact interaction. Introducing the ratio $g = (\alpha/\beta)^2$, these constants are

$$\eta_1 = 1 \tag{40}$$

$$A_1 = \frac{2\rho^2 + 4\rho + (3g+2)}{6(1+\rho)^2\alpha^2} \tag{41}$$

$$B_1 = A_1 \ , \tag{42}$$

$$\eta_2 = \left(\frac{12g}{7g+6}\right)^{3/2} \tag{43}$$

$$A_2 = \frac{(40g+3)\rho^2 + (32g+6)\rho + (21g^2+28g+3)}{6(7g+6)(1+\rho)^2\alpha^2} \tag{44}$$

$$B_2 = \frac{(-8g+1)\rho^2 + 2\rho + (7g^2+8g+1)}{2(7g+6)(1+\rho)^2\alpha^2} \ , \tag{45}$$

$$\eta_3 = \rho\left(\frac{6}{g+3}\right)^{3/2} \tag{46}$$

$$A_3 = \frac{(10g+6)\rho^2 + (8g+12)\rho + (7g+6)}{6(g+3)(1+\rho)^2\alpha^2} \tag{47}$$

$$B_3 = \frac{(-g+1)\rho^2 + 2\rho + (g+1)}{(g+3)(1+\rho)^2\alpha^2} \ , \tag{48}$$

$$\eta_4 = \rho\left(\frac{12g}{(2g+3)(g+2)}\right)^{3/2} \tag{49}$$

$$A_4 = \frac{(20g^2+40g+3)\rho^2 + (4g^2+14g+6)\rho + (5g^2+10g+3)}{6(2g+3)(g+2)(1+\rho)^2\alpha^2} \ , \tag{50}$$

$$B_4 = \frac{(-4g^2-8g+1)\rho^2 + (-4g^2-6g+2)\rho + (g^2+2g+1)}{2(2g+3)(g+2)(1+\rho)^2\alpha^2} \ . \tag{51}$$

These results were derived at MIT and ORNL [29] independently using MAPLE and MACSYMA algebra programs respectively.

Some important properties of these diagrams, specifically which are forward peaked or backward peaked processes, and which diagrams dominate at high energies, can be inferred by inspection. The leading diagram in the high energy limit is D_1, which is a forward peaked exponential in t. The other diagrams are exponentially suppressed in s and are also forward peaked, with the single exception of D_4. Note that for plausible values of $g \approx 1$ and $\rho \approx 0.6$ this diagram leads to a *backwards* peak ($B_4 < 0$). These properties have a simple common origin; since we are scattering through a hard delta function interaction, the only angular dependence comes from overlap suppression due to the spectator lines. A spectator line which is required to cross into the other hadron gives an especially large suppression at high energies and small angles. The amplitude for a crossing spectator line is maximum for backscattered hadrons; in this case the crossing spectator is actually continuing to move in a new hadron with the same momentum vector as the hadron it originally resided in.

The first diagram D_1 has no crossing spectators, so it is not suppressed in s; only the hard scattered constituents are required to cross into different hadrons. In diagrams D_2 and D_3 one spectator line is required to cross to a different hadron, so there is some suppression with increasing s. Since *two* spectators do not cross, they dominate the angular dependence, and the scattering is forward peaked. Diagram D_4, the backward peaking process, is qualitatively different because two spectator lines are required to change hadrons, and only one spectator does not cross. In this case "backwards" meson-baryon scattering actually corresponds to forward scattering for the two crossing spectator lines, which is obviously preferred. This description attributes backward peaks, which might otherwise appear counterintuitive, to the obvious mechanism of "minimum spectator suppression" at the quark level.

f) KN phase shifts and scattering lengths

Given the diagram weights (32-33) and our results (40-51) for the Gaussian overlap integrals, we have completed the derivation of the Hamiltonian matrix element h_{fi} for KN elastic scattering. Since we have used the same normalization for KN states as in our previous discussion of Kπ scattering [17] we can use the same relations derived there to relate h_{fi} to scattering variables. First we consider the elastic phase shifts, which are given by

$$\delta_\ell^{KN} = -\frac{2\pi^2 P_{cm} E_K E_N}{(E_K + E_N)} \int_{-1}^{1} h_{fi}^{KN} \, P_\ell(\mu) d\mu \ . \tag{52}$$

Using the integral $\int_{-1}^{1} e^{b\mu} P_\ell(\mu) d\mu = 2 i_\ell(b)$, we find

$$\delta_\ell^{KN} = -\frac{4\alpha_s}{3m_q^2} \frac{P_{cm} E_K E_N}{(E_K + E_N)} \sum_{i=1}^{4} w_i \, \eta_i \, \exp(-A_i P_{cm}^2) \, i_\ell(B_i P_{cm}^2) \ , \tag{53}$$

where one specifies the isospin state I=0 or I=1 through the choice of the diagram weights $\{w_i\}$.

As we approach the KN threshold the S-wave phase shift is asymptotically linear in P_{cm}, and the coefficient is the scattering length a_I. Since the exponential and the i_0 Bessel function are both unity in this limit, we recover a relatively simple result for the KN scattering length,

$$a_I^{KN} = -\frac{4\alpha_s}{3m_q^2} \frac{M_K M_N}{(M_K + M_N)} \sum_{i=1}^{4} w_i \, \eta_i \ . \tag{54}$$

Since the coefficients $\{\eta_i\}$ are relatively simple functions, we can write these scattering lengths as simple functions of α_s/m_q^2, $\rho = m_q/m_s$, the meson-baryon relative scale parameter $g = (\alpha/\beta)^2$ and the physical masses M_K and M_N. The results are

$$a_{I=1}^{KN} = -\frac{4\alpha_s}{3m_q^2}\frac{M_K M_N}{(M_K + M_N)}$$

$$\cdot \left[\frac{1}{3} + \frac{1}{18}\left(\frac{12g}{7g+6}\right)^{3/2} + \frac{1}{3}\,\rho\left(\frac{6}{g+3}\right)^{3/2} + \frac{1}{18}\,\rho\left(\frac{12g}{(2g+3)(g+2)}\right)^{3/2} \right] \qquad (55)$$

and

$$a_{I=0}^{KN} = -\frac{4\alpha_s}{3m_q^2}\frac{M_K M_N}{(M_K + M_N)}$$

$$\cdot \left[\frac{1}{6}\left(\frac{12g}{7g+6}\right)^{3/2} + \frac{1}{6}\,\rho\left(\frac{12g}{(2g+3)(g+2)}\right)^{3/2} \right] . \qquad (56)$$

The basic features of the low energy KN interaction, a repulsive I=1 S-wave and a repulsive but less strong I=0 S-wave, are already evident in these formulas. (The parameter $g = (\alpha/\beta)^2$ is constrained by quark model phenomenology to be comparable to unity.) Detailed numerical results for the scattering lengths and phase shifts and a comparison with experiment are presented in the next section.

III. COMPARISON WITH EXPERIMENT

a) Scattering lengths

Before we discuss our numerical predictions we first review the status of the experimental scattering lengths. Since there are unresolved disagreements between analyses in the I=0 channel, we have compiled relatively recent (since 1980) single-energy S-wave phase shifts for our discussion. These are in chronological order Martin and Oades [30] (Aarhus and UC London, 1980); Watts *et al.* [31] (QMC and RAL, 1980); Hashimoto [32] (Kyoto and VPI, 1984); and Hyslop *et al.* [5] (VPI, 1992). The I=1 data set analysed by Arndt and Roper [33] (VPI, 1985) was incorporated in the 1992 VPI simultaneous analysis of I=0 and I=1 data, so we shall not consider it separately. The energy dependent parametrizations of Corden *et al.* [34] and Nakajima *et al.* [35] are not included in our discussion.

In Fig.1 we show these experimental I=0 and I=1 S-wave phase shifts versus $P_{cm} = |\vec{P}_{cm}|$. The linear low energy behavior which determines the scattering length is evident in the I=1 data, and Hyslop *et al.* cite a fitted value of $a_{I=1}^{KN} = -0.33$ fm. Previous analyses (summarized in [1] and [5]) have given values between $-0.28(6)$ fm [36] and -0.33 fm [5,37]. A more useful way to present the S-wave phase shift data is to display δ_0^I/P_{cm} versus P_{cm}^2; the intercept is the scattering length, and the slope at intercept determines the effective range. In Fig.2 we show the S-wave phase shifts in this manner; an I=1 scattering length of about $-0.31(1)$ fm is indeed evident, which we shall take as our estimated experimental value.

Unfortunately the I=0 scattering length is much less well determined, as is evident in Figs.1 and 2. Previous (favored) solutions up to 1982 are summarized in Table 2.3 of [1], and range between $+0.02$ fm and $-0.11^{+0.06}_{-0.04}$ fm. There appear to be two sets of low energy values in the data of Fig.1, a smaller phase shift from the Aarhus-UCL and QMC-RAL collaborations and a larger one from from the Kyoto-VPI and VPI analyses. Below $P_{cm} = 0.4$ Gev the Kyoto-VPI and VPI results are larger than Aarhus-UCL and QMC-RAL by about a factor of two. The VPI group actually cite a scattering length of $a^{KN}_{I=0} = 0.0$ fm, although this requires rapid low energy variation below the first experimental point (compare their Fig.1(a) with the I=1 phase shift in their Fig.2(a), which is constrained by experiment at lower energy and shows the expected $\sqrt{T_{lab}} \propto P_{cm}$ S-wave dependence). Since the I=1 phase shift is close to linear for $P_{cm} < 0.4$ Gev ($k_{lab} < 0.7$ Gev), we will assume that the zero I=0 scattering length quoted in [5] is an artifact of their fit, and that the actual I=0 phase shift is approximately linear in P_{cm} for $P_{cm} < 0.4$ Gev. We can then read the I=0 scattering length from the intercept in Fig.2. From the figure we see that a naive extrapolation to threshold leads to scattering lengths of about $-0.09(1)$ fm and $-0.17(2)$ fm respectively from the two sets of references. In summary, the experimental phase shifts shown in Fig.2 suggest to us the scattering lengths

$$\begin{aligned} a^{KN}_{I=1}(expt.) &= -0.31(1) \text{ fm} \; ; \\ a^{KN}_{I=0}(expt.)\Big|_{Aarhus-QMC-RAL-UCL} &= -0.09(1) \text{ fm} \; , \\ a^{KN}_{I=0}(expt.)\Big|_{Kyoto-VPI} &= -0.17(2) \text{ fm} \; . \end{aligned} \tag{57}$$

We emphasize that the I=0 values are our interpretation of the data from Fig.2, and the references cited quote smaller scattering lengths that we believe the data does not support. As the values of the I=0 scattering length and low energy phase shifts are controversial, an accurate determination should be a first priority at a kaon facility.

To compare our predictions with experiment we first use a "reference parameter set" with conventional quark model parameters. The hyperfine strength is taken to be $\alpha_s/m_q^2 = 0.6/(0.33)^2$ Gev^{-2}, and the nonstrange to strange quark mass ratio is $\rho = m_q/m_s = 0.33$ Gev $/0.55$ Gev $= 0.6$. The remaining parameter in the scattering length formulas is $g = (\alpha/\beta)^2$, the ratio of baryon to meson width parameters squared. These parameters are rather less well determined phenomenologically. For baryons, values in the range $\alpha = 0.25 - 0.41$ Gev have been used in nonrelativistic quark model studies [38–40]. Isgur and Karl [41] originally used $\alpha = 0.32$ Gev for spectroscopy, but Copley, Karl and Obryk [42] had earlier found that the photocouplings of baryon resonances required a somewhat larger value of $\alpha = 0.41$ Gev, which may be a more realistic estimate [38,39] because it is less sensitive to short distance hyperfine matrix elements. This larger value was also found by Koniuk and Isgur [43] for baryon electromagnetic transition amplitudes. Here we take $\alpha = 0.4$ Gev as our reference value. For mesons, studies of various matrix elements have led to values of $\beta = 0.2 - 0.4$ Gev [39]. In our previous study of I=2 $\pi\pi$ scattering we found a best fit to the S-wave phase shift data with $\beta = 0.337$ Gev. Here we use a similar $\beta = 0.35$ Gev as our reference value; if the quark Born formalism is realistic we should use essentially the same meson parameters in all reactions.

With our reference parameter set and physical masses $M_K = 0.495$ Gev and $M_N = 0.940$ Gev, our formulas (55) and (56) give

$$a^{KN}_{I=1}(ref.\ set) = -0.35 \text{ fm} \tag{58}$$

and

$$a^{KN}_{I=0}(ref.\ set) = -0.12 \text{ fm} \ . \tag{59}$$

In view of our approximations, the parameter uncertainties, and the uncertainties in the I=0 data, these scattering lengths compare rather well with experiment. Note that our conclusions differ from those of Bender *et al.* [24], who reported that the OGE contribution to I=1 scattering was too small to explain the observed S-wave phase shift. We discuss this disagreement further in the appendix.

Now suppose we attempt to fit our estimated experimental values of the scattering lengths (57) by varying our parameter set. It is useful to fit the ratio $a^{KN}_{I=0}/a^{KN}_{I=1}$, since this involves only ρ and the width parameter g. We have fixed $\rho = 0.6$, and in any case we find that $a^{KN}_{I=0}/a^{KN}_{I=1}$ is insensitive to ρ, so only g remains as an important parameter. In Fig.3 we show the predicted ratio of KN scattering lengths as a function of α/β. The two experimental ratios assuming the values in (57) are also indicated. The larger ratio $a^{KN}_{I=0}/a^{KN}_{I=1} = 0.17/0.31$ requires $\alpha/\beta = 1.91$, rather far from typical quark model values. Fitting the smaller ratio $a^{KN}_{I=0}/a^{KN}_{I=1} = 0.09/0.31$ requires $\alpha/\beta = 1.02$, which is more representative of quark model parameters. An accurate determination of the I=0 KN scattering length through direct low energy measurements, rather than by extrapolation, would be a very useful experimental contribution; this would allow a more confident test of our results and those of other models (as shown for example in Table 6-4 of Hyslop [37]).

b) S-wave phase shifts

The S-wave KN phase shifts predicted by (53) with $\ell = 0$ given the "reference parameter set" $\alpha_s/m_q^2 = 0.6/(0.33)^2$ Gev^{-2}, $\rho = m_q/m_s = 0.6$, $\alpha = 0.4$ Gev and $\beta = 0.35$ Gev are shown as dashed lines in Fig.4. As we noted in the previous section, this parameter set gives reasonable scattering lengths, although the I=0 scattering length is not yet very well established experimentally.

At higher energies the reference parameter set predicts an I=1 phase shift that retreats more quickly with energy than is observed experimentally; in Fig.4 we see a rapid departure of theory and experiment above $P_{cm} = 0.4$ Gev ($k_{lab} = 0.7$ Gev). This is near the opening of the inelastic channels KΔ and K*N, as indicated in Fig.4. Two possible reasons for this discrepancy are 1) inelastic effects of the channels KΔ, K*N and K$^*\Delta$, which should become important just where theory and experiment part, and 2) short distance components in the meson and baryon wavefunctions that are underestimated by the smooth Gaussian wavefunctions (2) and (4).

Although inelastic effects are certainly important experimentally [3,4], the most important low energy inelastic process is P-wave KΔ production [4]. Hyslop *et al.* [5] similarly find relatively small inelasticities in the I=1 KN S-wave, with $\eta \geq 0.9$ for $P_{cm} \leq 0.68$ Gev. At the end of this range our predicted phase shift given the reference parameter set is only about half the observed value, so it appears unlikely that the discrepancy is mainly due to inelastic channels.

A second possible reason for the discrepancy is a departure of the hadron wavefunctions from the assumed single Gaussian forms at short distances; both the meson $q\bar{q}$ states and the baryon qq substates experience attractive short distance interactions from the color Coulomb and hyperfine terms (for spin singlets), which will lead to enhancements of the short distance components of their wavefunctions and increased high energy scattering amplitudes. If this is the principal reason for the discrepancy, we would expect a global fit to the S-wave phase shifts to prefer a smaller hadron length scale. In Fig.4 we show the result of a three-parameter fit to the full 1992 VPI I=0,1 energy independent S-wave data set [5], letting $\alpha_s/m_q^2, \alpha$ and β vary and holding $\rho = 0.6$ fixed. The fit is shown as solid lines, and is evidently quite reasonable both near threshold and at higher energies. The fitted parameters are $\alpha_s/m_q^2 = 0.59/(0.33)^2$ Gev^{-2}, $\alpha = 0.68$ Gev and $\beta = 0.43$ Gev; the hyperfine strength is a typical quark model result but the width parameters α and β are about 1.5 times the usual quark model values. Thus, a fit to the S-wave VPI data using single Gaussian wavefunctions requires a hadron length scale about 0.7 times the usual scale. This result is largely independent of the data set chosen, since it is driven by the large I=1 phase shift, which shows little variation between analyses. Evidently the predicted S-wave phase shifts at higher energies are indeed very sensitive to the short distance parts of the wavefunction; this supports our conjecture that the discrepancy at higher energies is an artifact of our single Gaussian wavefunctions. A calculation of these S-wave phase shifts using realistic Coulomb plus linear plus hyperfine wavefunctions is planned [38] and should provide a very interesting test of the quark Born formalism.

c) Higher-L partial waves, spin-orbit and inelastic effects

In addition to the S-wave phase shifts, higher-L KN elastic phase shifts and properties of the inelastic reactions KN→K*N, KN→KΔ and KN→K*Δ have been the subjects of experimental investigations. These studies have found important effects in the L>0 partial waves which are beyond the scope of the present paper.

One especially interesting effect is a remarkably large spin-orbit interaction in the I=0 KN system; the L=1 states have a large, positive phase shift for J=1/2 and a weaker, negative phase shift for J=3/2 (see [5] and references cited therein). This spin-orbit interaction cannot arise in our quark Born amplitudes given the approximations we have made in this paper; since we have incorporated only the spin-spin hyperfine interaction in single hadronic channels, our phase shifts (53) are functions of the total hadronic L and S but not J. Some but not all of this spin-orbit interaction may simply require incorporation of the OGE spin-orbit term; Mukhopadhyay and Pirner [27] found that the quark spin-orbit interaction was sufficient to explain the sign and magnitude of some of the weaker KN spin-orbit forces, but that the I=0, J=1/2 phase shift was much too large to be explained as an OGE force. The strong KN spin-orbit forces might conceivably be due to couplings to inelastic channels; since the available mixing states and their couplings to KN are J-dependent, they might lead to effective spin-orbit forces at the hadronic level, even if we do not include spin-orbit forces at the quark level. We hope to treat this interesting possibility in a future study of coupled channel effects using the quark Born formalism.

Since we do not have a model of the large spin-orbit effect it is not appropriate to include a detailed discussion of our predicted amplitudes and cross sections at higher energies, where higher partial waves are important. In the interest of completeness however we will briefly discuss our predicted differential cross section at high energy, since we previously noted that we found an exponential in t in I=2 $\pi\pi$ scattering, reminiscent of diffraction in magnitude but not in phase [16]. The differential cross section in this unequal mass case is related to the h_{fi} matrix element (29) by

$$\frac{d\sigma}{dt} = 4\pi^5 \frac{\Big[s^2 - (M_N^2 - M_K^2)^2 \Big]^2}{s^2 \Big[(s - (M_N + M_K)^2)(s - (M_N - M_K)^2) \Big]} \, |h_{fi}|^2 \ . \tag{60}$$

For KN scattering in the high energy limit only the contribution from diagram D_1 (20) survives, and we find

$$\lim_{s \to \infty} \frac{d\sigma}{dt} = \frac{4\pi\alpha_s^2}{9m_q^4} \, w_1^2 \, \exp\{A_1 t\} \ . \tag{61}$$

Thus we again find an exponential in t at high energy, with a slope parameter (41) that is numerically equal to

$$b = A_1 = 3.7 \ \mathrm{Gev}^{-2} \tag{62}$$

given our reference parameter set. This is similar to the observed diffractive I=1 KN slope parameter [44] of

$$b(expt.) \approx 5.5 - 5.9 \ \mathrm{Gev}^{-2} \ . \tag{63}$$

The normalizations of the theoretical and experimental I=1 high energy differential cross sections however differ by about an order of magnitude, and are 1.8 mb Gev^{-2} (reference parameter set) versus $\approx$ 15 mb Gev^{-2} (experiment [44]). We noted a similar tendency for the reference parameter set to underestimate high energy amplitudes in our discussion of the S-wave phase shifts, which we attributed to the single Gaussian wavefunction approximation. One interesting prediction is that I=0 KN scattering should have no diffractive peak in the high energy limit, since it has has $w_1 = 0$; unfortunately there is no I=0 high energy data to compare this prediction with. A serious comparison with high energy scattering will presumably require the use of wavefunctions with more realistic high momentum components as well as the incorporation of inelastic channels, which may strongly affect the elastic amplitudes.

IV. KN EQUIVALENT POTENTIALS

Sufficiently close to threshold our quark Born scattering amplitudes can be approximated by local potentials. These potentials are useful in applications such as multichannel scattering and investigations of possible bound states, which are easiest to model using a Schrödinger equation formalism with local potentials. There are many ways to define an equivalent low energy potential from a scattering amplitude such as h_{fi}; several such procedures are discussed in [18,45] and in Appendix E of [16]. Of course effective potentials extracted using different definitions can appear to be very different functions of r although they lead to similar low energy scattering amplitudes.

One approach to defining an equivalent potential is to derive a potential operator $V_{op}(r)$ which give the scattering amplitude h_{fi} in Born approximation. This "Born-equivalent potential" technique is discussed in reference [45] and in Appendix E of [16]; it has been tested on the OGE interaction, from which one recovers the correct Breit-Fermi Hamiltonian at $O(v^2/c^2)$ [45]. To derive the Born-equivalent potential we reexpress our scattering amplitude in the CM frame as a function of the transferred three-momentum $\vec{q} = \vec{C} - \vec{A}$ and an orthogonal variable $\vec{\mathcal{P}} = (\vec{A} + \vec{C})/2$. We then expand the scattering amplitude in a power series in $\vec{\mathcal{P}}$ and equate the expansion to the Born expression for nonrelativistic potential scattering through a general potential operator $V_{op}(r)$, which may contain gradient operators. The leading term, of order $\mathcal{P}^0$, gives the Born-equivalent local potential $V(r)$.

In this meson-baryon scattering problem our Hamiltonian matrix elements are of the form

$$h_{fi} = \frac{8\pi\alpha_s}{3m_q^2} \frac{1}{(2\pi)^3} \sum_{i=1}^{4} w_i \eta_i \exp\Big\{ -(A_i - B_i\mu) P_{cm}^2 \Big\} \, . \tag{64}$$

Making the required substitutions $P_{cm}^2 = \vec{\mathcal{P}}^2 + \vec{q}^{\,2}/4$ and $P_{cm}^2 \mu = \vec{\mathcal{P}}^2 - \vec{q}^{\,2}/4$ and Fourier transforming with respect to $\vec{q}$ as in [16] gives the equivalent low energy KN potential

$$V_{KN}(r) = \frac{8\alpha_s}{3\sqrt{\pi} m_q^2} \sum_{i=1}^{4} \frac{w_i \eta_i}{(A_i + B_i)^{3/2}} \exp\Big\{ -r^2/(A_i + B_i) \Big\} \, . \tag{65}$$

Thus our Born-equivalent meson-baryon potentials are sums of four Gaussians, one from each inequivalent quark Born diagram, weighted by the diagram weights of that channel.

The potentials for I=0 and I=1 with our reference parameter set $\alpha_s = 0.6$, $m_q = 0.33$ Gev, $\rho = m_q/m_s = 0.6$, $\alpha = 0.40$ Gev and $\beta = 0.35$ Gev are shown in Fig.5. They are repulsive and have a range of about 0.3 fm, as one would expect for a short range "nuclear" core. The potentials at contact are rather similar in this formalism, and the relative weakness of I=0 scattering is a result of its shorter range. This is an effect of the backward peaking diagram D_4, which leads to a very short range potential with a large value at contact, and carries higher weight in I=0 scattering.

Although these Born-equivalent potentials are convenient for use in a meson-baryon Schrödinger equation, the actual KN potentials are so strong that they reproduce some features of the interaction only qualitatively. For example, the Born diagrams give an I=1 scattering length of -0.35 fm, but the Born-equivalent potential (65) for I=1 in the Schrödinger equation for KN leads to a scattering length of only about -0.22 fm. The discrepancy is due to higher order effects of $V_{KN}(r)$ in the Schrödinger equation; we have confirmed that the ratio of h_{fi} and $V_{KN}(r)$ scattering lengths approaches unity in the small-α_s limit. In a multichannel study one might modify $V_{KN}(r)$ (65) to give the input h_{fi} scattering lengths, perhaps through a change in the overall normalization, as a way of providing a more realistic potential model of the quark Born amplitudes.

V. RESULTS FOR KΔ, K*N AND K$^*\Delta$; PROSPECTS FOR Z*-MOLECULES

The channels KΔ, K*N and K$^*\Delta$ are interesting in part because they may support molecular bound states if the effective interaction is sufficiently attractive. In contrast the low energy KN interaction is repulsive in both isospin states. These "Z*-molecules" would appear experimentally as resonances with masses somewhat below the thresholds of ≈ 1.7 Gev, ≈ 1.85 Gev and ≈ 2.1 Gev. Even if there are no bound states, attractive interactions will lead to threshold enhancements which might be misidentified as Z* resonances just above threshold.

Plausible binding energies of hadronic molecules can be estimated from the uncertainty principle and the minimum separation allowed for distinct hadrons as $E_B \sim 1/(M_{had} \cdot 1\,\mathrm{fm}^2) \sim 50$ Mev. In comparison, the best established molecules or molecule candidates have binding energies ranging from 2.2 Mev (the deuteron, which has a repulsive core) through 10-30 Mev (the $f_0(975)$, $a_0(980)$ and $\Lambda(1405)$). (The $f_0(1710)$, with a binding energy relative to K$^*\bar{\mathrm{K}}^*$ of about 75 Mev, appears plausible but is a more controversial candidate [13].) Finally, the state $f_2(1520)$ seen by the Asterix [46], Crystal Barrel [47] and Obelix [48] collaborations in P$\bar{\mathrm{P}}$ annihilation is an obvious candidate for a nonstrange vector-vector molecule, with a (poorly determined) binding energy relative to $\rho\rho$ threshold of perhaps 20 Mev.

Several candidate Z* resonances which might be meson-baryon molecule states have been reported in KN partial wave analyses. The 1986 Particle Data Group compilation [49] (the most recent to review the subject of Z* resonances) cited two I=0 candidates, $[Z_0(1780), \frac{1}{2}^+]$ and $[Z_0(1865), \frac{3}{2}^-]$ and four I=1 possibilities, $[Z_1(1725), \frac{1}{2}^+]$; $[Z_1(1900), \frac{3}{2}^+]$; $Z_1(2150)$ and $Z_1(2500)$. However the evidence for these states is not strong, and the PDG argue that the standards of proof must be strict in this exotic channel. For this reason these states were only given a one star "Evidence weak; could disappear." status. The 1986 PDG also noted that "The general prejudice against baryons not made of three quarks and the lack of any experimental activity in this area make it likely that it will be another 15 years before the issue is decided.". The 1992 PDG compilation [50] makes a similar statement, with "15 years" revised to "20 years".

In their recent analysis of the data Hyslop *et al.* [5] summarize some previous claims and report evidence for "resonancelike structures" $[Z_0(1831), \frac{1}{2}^+]$; $[Z_0(1788), \frac{3}{2}^-]$; $[Z_1(1811), \frac{3}{2}^+]$ and $[Z_1(2074), \frac{5}{2}^-]$. The negative parity candidates $Z_0(1788)$ and $Z_1(2074)$ have quantum numbers and masses consistent with S-wave K*N and K$^*\Delta$ molecules respectively. We would not normally expect P-wave molecules; odd-L is required to couple to positive parity KN channels, and the centrifical barrier suppresses binding due to these short range forces. However, threshold effects which resemble resonances might arise in the full multichannel problem, and the very strong spin-orbit force evident in the P$_{01}$ and P$_{03}$ KN partial waves may be sufficient to induce binding in some channels. A clarification of the status of Z* candidates through the determination of experimental amplitudes for the processes KN $\to$ K*N, KN $\to$ KΔ and KN $\to$ K$^*\Delta$ in addition to the elastic KN reaction will be an important goal of future studies at kaon factories.

All the S-wave (I,J$^{\mathrm{P}}$) quantum numbers, in which molecule bound states are *a priori* most likely, are as follows;

$$\mathrm{K}\Delta(\approx 1.6-1.7\ \mathrm{Gev}): \quad (2,\frac{3}{2}^-)\,;(1,\frac{3}{2}^-)\,;$$

$$\mathrm{K}^*\mathrm{N}(\approx 1.75-1.85\ \mathrm{Gev}): \quad (1,\frac{3}{2}^-)\,;(1,\frac{1}{2}^-)\,; \qquad (0,\frac{3}{2}^-)\,;(0,\frac{1}{2}^-)\,;$$

$$\mathrm{K}^*\Delta(\approx 2.0-2.1\ \mathrm{Gev}): \quad (2,\frac{5}{2}^-)\,;(2,\frac{3}{2}^-)\,;(2,\frac{1}{2}^-)\,; \qquad (1,\frac{5}{2}^-)\,;(1,\frac{3}{2}^-)\,;(1,\frac{1}{2}^-)\,.$$

We can use our detailed model of meson-baryon scattering in the $(q\bar{s})(qqq)$ system ($q = u, d$) to identify channels which experience attractive interactions as a result of the color hyperfine term. These we again show as weight factors which multiply each of the four diagrams $D_1 \ldots D_4$. Since the overlap integrals these weights multiply are all positive and of comparable magnitude, the summed weight can be used as an estimate of the sign and relative strength of the interaction in each channel. Positive weights correspond to a repulsive interaction. Our results for the h_{fi} "diagram weights" for all KΔ, K*N and K$^*\Delta$ channels in (I,S$_{tot}$) notation are given below. We also give the numerical values we find for the scattering length in each channel given our reference parameter set and masses $\mathrm{M}_{K^*} = 0.895$ Gev and $\mathrm{M}_\Delta = 1.210$ Gev.

$$\mathrm{K}\Delta(2,\frac{3}{2}) = \frac{1}{6}\left[\ +3,\ -1,\ +3,\ -1\ \right]\,; \tag{66}$$

$$a = -0.38\ \ \mathrm{fm}\ . \tag{67}$$

$$\mathrm{K}\Delta(1,\frac{3}{2}) = -\frac{1}{3}\ \mathrm{K}\Delta(2,\frac{3}{2}) = \frac{1}{18}\left[\ -3,\ +1,\ -3,\ +1\ \right]\,; \tag{68}$$

$$a = +0.13\ \ \mathrm{fm}\ . \tag{69}$$

$$\mathrm{K}^*\mathrm{N}(1,\frac{3}{2}) = \frac{1}{27}\left[\ +7,\ +1,\ -5,\ 0\ \right]\,; \tag{70}$$

$$a = -0.08\ \ \mathrm{fm}\ . \tag{71}$$

$$\mathrm{K}^*\mathrm{N}(1,\frac{1}{2}) = \frac{1}{54}\left[\ +26,\ +5,\ +2,\ -3\ \right]\,; \tag{72}$$

$$a = -0.39\ \ \mathrm{fm}\ . \tag{73}$$

$$\mathrm{K}^*\mathrm{N}(0,\frac{3}{2}) = \frac{1}{9}\left[\ +1,\ +1,\ +1,\ 0\ \right]\,; \tag{74}$$

$$a = -0.22 \ \ \mathrm{fm}\ . \tag{75}$$

$$\mathrm{K}^*\mathrm{N}(0,\frac{1}{2}) = \frac{1}{18}\ \Big[-4,\ +5,\ -4,\ -3 \Big]\ ; \tag{76}$$

$$a = +0.15 \ \ \mathrm{fm}\ . \tag{77}$$

$$\mathrm{K}^*\Delta(2,\frac{5}{2}) = \frac{1}{3}\ \Big[+1,\ -1,\ -1,\ +1 \Big]\ ; \tag{78}$$

$$a = +0.14 \ \ \mathrm{fm}\ . \tag{79}$$

$$\mathrm{K}^*\Delta(2,\frac{3}{2}) = \frac{1}{18}\ \Big[+11,\ -1,\ -1,\ -9 \Big]\ ; \tag{80}$$

$$a = -0.20 \ \ \mathrm{fm}\ . \tag{81}$$

$$\mathrm{K}^*\Delta(2,\frac{1}{2}) = \frac{1}{9}\ \Big[+7,\ +1,\ +1,\ +3 \Big]\ ; \tag{82}$$

$$a = -0.86 \ \ \mathrm{fm}\ . \tag{83}$$

$$\mathrm{K}^*\Delta(1,S_{tot}) = -\frac{1}{3}\ \mathrm{K}^*\Delta(2,S_{tot}) \qquad \forall\ S_{tot}\ ; \tag{84}$$

$$\mathrm{K}^*\Delta(1,\frac{5}{2}) = \frac{1}{9}\ \Big[-1,\ +1,\ +1,\ -1 \Big]\ ; \tag{85}$$

$$a = -0.05 \ \ \mathrm{fm}\ . \tag{86}$$

$$\mathrm{K}^*\Delta(1,\frac{3}{2}) = \frac{1}{54}\ \Big[-11,\ +1,\ +1,\ +9 \Big]\ ; \tag{87}$$

$$a = +0.07 \ \ \mathrm{fm}\ . \tag{88}$$

$$\mathrm{K}^*\Delta(1,\frac{1}{2}) = \frac{1}{27}\ \Big[-7,\ -1,\ -1,\ -3 \Big]\ ; \tag{89}$$

$$a = +0.29 \ \ \mathrm{fm}\ . \tag{90}$$

Evidently attractive forces arise from the OGE spin-spin interaction in the minimum-spin, minimum-isospin channels,

$$\mathrm{K}\Delta : \quad (1, \frac{3}{2}) \ ;$$

$$\mathrm{K}^*\mathrm{N} : \quad (0, \frac{1}{2}) \ ;$$

$$\mathrm{K}^*\Delta : \quad (1, \frac{1}{2}) \ .$$

The two exceptions to this rule are the K*Δ channels

$$\mathrm{K}^*\Delta : \quad (2, \frac{5}{2})$$

and

$$\mathrm{K}^*\Delta : \quad (1, \frac{3}{2}) \ ;$$

although their weights sum to zero, variations in the detailed overlap integrals lead to attractive OGE-hyperfine forces in these two channels as well.

For our reference parameter set we find no molecular bound states; the attractive forces are too weak to induce binding. The experimental situation at present is rather confused; some references claim evidence for resonances in several channels (see for example [5,32,37]), whereas other references such as [30] and [31] conclude that the same phase shifts are non-resonant. Our results do not support the most recent claims of resonances [5], since the S-wave quantum numbers of our attractive channels do not correspond to those of the negative parity candidates $[Z_0(1788), \frac{3}{2}^-]$ and $[Z_1(2074), \frac{5}{2}^-]$. However our negative result may be an artifact of our approximations, including the neglect of spin-orbit effects and couplings between channels. The spin-orbit effects are known from experiment to be very important, and might be sufficient to lead to Z*-molecule bound states or strong threshold enhancements in the attractive channels. Our negative result is based on strong assumptions on the form of the interaction; this should be relaxed in future theoretical work, and should not be used to argue against experimental searches for possible Z* meson-baryon molecules.

VI. SUMMARY AND CONCLUSIONS

In this paper we have applied the quark Born diagram formalism to KN scattering. In this approach one calculates hadron-hadron scattering amplitudes in the nonrelativistic quark potential model assuming that the amplitude is the coherent sum of all OGE interactions followed by all allowed quark line exchanges; this is expected to be a useful description of reactions which are free of $q\bar{q}$ annihilation. The model has few parameters, here α_s/m_q^2, $\rho = m_q/m_s$ and the hadron wavefunction parameters, and with Gaussian wavefunctions the scattering amplitudes can be derived analytically. The model was previously applied to I=2 $\pi\pi$ and I=3/2 Kπ scattering with good results.

KN scattering is an important test of this approach because it is also annihilation-free (at the valence quark level) and the meson and baryon wavefunction parameters and the interaction strength are already reasonably well established. Thus there is little freedom to adjust parameters. We find good agreement with the experimental low energy I=0 and I=1 phase shifts given standard quark model parameters. (The experimental I=0 scattering length is usually claimed to be very small; we disagree with this interpretation of the data and argue in support of a larger value.) A resolution of the disagreements between different I=0 KN phase shift analyses, especially at very low energies, is an important task for future experimental work. Hyslop [37] also suggests additional experimental work on the I=0 KN system. At higher energies we find that the single Gaussian S-wave phase shifts fall with energy more quickly than experiment given standard quark model parameters; we attribute most of this effect to departures of the hadron wavefunction from single Gaussians at short distances, perhaps in response to the attractive color hyperfine interaction. We have confirmed that a smaller hadronic length scale (about 0.7 times the usual nonrelativistic quark potential model scale) gives S-wave phase shifts which are in good agreement with experiment at all energies.

We have investigated the possibility of Z^*-molecule meson-baryon bound states by extending our calculations to all channels allowed for $K\Delta$, K^*N and $K^*\Delta$. Although we do find attractive interactions in certain channels, in no case is the corresponding interhadron potential sufficiently strong to form a bound state. Of course this result may be an artifact of our approximations, in particular the assumption of keeping only the spin-spin color hyperfine term and the single channel approximation. The effect of relaxing these approximations would be a very interesting topic for future study.

There are additional effects in the L>0 KN system which are known to be important experimentally, which are not incorporated in our calculations of single channel color hyperfine matrix elements. The most important of these is a very large spin-orbit force, which it has not been possible to explain as an OGE interaction [22,27]. Both this spin-orbit interaction and the Z^* candidates may be strongly affected by coupled channel effects, which we plan to investigate in future work. Since much is already known experimentally about the reactions $KN \to K^*N$ and $KN \to K\Delta$, it should be possible to test predictions of the quark Born diagrams for these channel couplings using existing data sets. Although one might expect OPE forces to be important in coupling KN to inelastic channels, such as in I=1 $KN \to K^*N$, the OPE contribution to this process has been found experimentally to be small near threshold [4]. Thus experiment suggests that interquark forces such as OGE and the confining interaction may be more important than meson exchange in coupling KN to inelastic channels. We plan to evaluate these offdiagonal couplings in detail in a future study.

ACKNOWLEDGMENTS

We acknowledge useful contributions from R.Arndt, W.Bugg, S.Capstick, F.E.Close, G.Condo, H.Feshbach, N.Isgur, R.Koniuk, M.D.Kovarik, K.Maltman, B.R.Martin, D.Morgan, G.C.Oades, R.J.N.Phillips, B.Ratcliff, R.G.Roberts, L.D.Roper, D.Ross, S.Sorensen, J.Weinstein and R.Workman. This work was sponsored in part by the United States Department of Energy under contracts DE-AC02-76ER03069 with the Center for Theoretical Physics at the Massachusetts Institute of Technology and DE-AC05-840R21400

with Martin Marietta Energy Systems Inc.

REFERENCES

1 C.B.Dover and G.E.Walker, Phys. Rep. 89, 1 (1982).

2 See for example S.Nagamiya, in *Quark Matter '91: Proceedings of the Ninth International Conference on Ultra-Relativistic Nucleus-Nucleus Collisions* (Gatlinburg, TN 11-15 November 1991), eds. T.C.Awes, F.E.Obenshain, F.Plasil, M.R.Strayer and C.Y.Wong, (North-Holland, 1992), pp.5c-25c; W.A.Zajc, *ibid.*, pp.237c-254c.

3 R.W.Bland, M.G.Bowler, J.L.Brown, J.A.Kadyk, G.Goldhaber, S.Goldhaber, V.H.Seeger and G.H.Trilling, Nucl. Phys. B13, 595 (1969).

4 R.W.Bland, M.G.Bowler, J.L.Brown, G.Goldhaber, S.Goldhaber, J.A.Kadyk, V.H.Seeger and G.H.Trilling, Nucl. Phys. B18, 537 (1970).

5 J.S.Hyslop, R.A.Arndt, L.D.Roper and R.L.Workman, Phys. Rev. D46, 961 (1992).

6 P.M.Gensini and G.Violini, in *Proceedings of the International Symposium on Hypernuclear and Strange Particle Physics* (Shimoda, Japan 9-12 December 1991), Universitá di Perugia report DFUPG-36-91-rev (February 1992).

7 J.Lee-Franzini, Frascati report LNF-92/046(P) (1992).

8 See for example J.J.deSwart, P.J.Mulders and L.J.Somers, "Multi-quark Baryons", in *Proceedings of the IVth International Conference on Baryon Resonances "Baryon 1980"* (Toronto, 14-16 July 1980), ed. N.Isgur, (University of Toronto Press, 1981) p.405.

9 See for example R.L.Jaffe, Phys. Rev. D15, 267 (1977).

10 R.L.Jaffe, Phys. Rev. Lett. 38, 195, 617E (1977).

11 N.Isgur, Acta Physica Austriaca, Suppl. XXVII, 177-266 (1985).

12 J.Weinstein and N.Isgur, Phys. Rev. Lett. 48, 659 (1982); Phys. Rev. D27, 588 (1983); Phys. Rev. D41, 2236 (1990); Phys. Rev. D43, 95 (1991).

13 Yu.S.Kalashnikova, in *Proceedings of the IVth International Conference on Hadron Spectroscopy "Hadron '91"* (College Park, Md. 12-16 August 1991), (World Scientific, 1992), pp.777-782; K.Dooley, *ibid.*, pp. 789-794; N.Törnqvist, *ibid.*, pp.795-798; Phys. Rev. Lett. 67, 556 (1991); K.Dooley, E.S.Swanson, and T.Barnes, Phys. Lett. 275B, 478 (1992); K.Dooley, University of Toronto Ph.D. thesis (in preparation).

14 See for example J.F.Gunion *et al.*, Phys. Rev. D8, 287 (1973); G.P.Lepage and S.J.Brodsky, Phys. Rev. D22, 2157 (1980); G.Farrar, Phys. Rev. Lett. 53, 28 (1984); S.J.Brodsky and G.P.Lepage, in *Perturbative Quantum Chromodynamics*, ed. A.Muller (World Scientific, 1989).

15 B.R.Baller, Phys. Rev. Lett. 60, 1118 (1988).

16 T.Barnes and E.S.Swanson, Phys. Rev. D46, 131 (1992).

17 T.Barnes, E.S.Swanson and J.Weinstein, Phys. Rev. D46, 4868 (1992).

18 E.S.Swanson, "Inter-meson Potentials from the Constituent Quark Model", MIT report MIT-CTP-2047 (1992), to appear in Ann. Phys. (NY) 219 (1992).

19 A.C.Davis, W.N.Cottingham and J.W.Alcock, Nucl. Phys. B111, 233 (1976); J. Phys. G4, 323 (1978); R.Büttgen, K.Holinde and J.Speth, Phys. Lett. 163B, 305 (1985).

20 R.L.Jaffe and F.E.Low, D19, 2105 (1979).

21 C.Roiesnel, Phys. Rev. D20, 1646 (1979).

22 E.A.Veit, A.W.Thomas and B.K.Jennings, Phys. Rev. D31, 2242 (1985).

23 I.Bender and H.G.Dosch, Z. Phys. C13, 69 (1982).

24 I.Bender, H.G.Dosch, H.J.Pirner and H.G.Kruse, Nucl. Phys. A414, 359 (1984).

25 R.K.Campbell and D.Robson, Phys. Rev. D36, 2682 (1987).

[26] H.J.Pirner and B.Povh, Phys. Lett. 114B, 308 (1982).
[27] D.Mukhopadhyay and H.J.Pirner, Nucl. Phys. A442, 605 (1985).
[28] D.A.Liberman, Phys. Rev. D16, 1542 (1977); C.E.DeTar, Phys. Rev. D17, 302 (1977); *ibid.*, p.323; M.Oka and K.Yazaki, Phys. Lett. 90B, 41 (1980); Prog. Theor. Phys. 66, 556 (1981); *ibid.*, p.572; A.Faessler, F.Fernandez, G.Lubeck and K.Shimizu, Phys. Lett. 112B 201 (1982); K.Maltman and N.Isgur, Phys. Rev. Lett. 50, 1827 (1983); M.Oka and C.J.Horowitz, Phys. Rev. D31, 2773 (1985); Y.Koike, Nucl.Phys. A454, 509 (1986); K.Shimizu, Rep. Prog. Phys. 52, 1 (1989); Yu.A.Kuperin, S.B.Levin and Yu.B.Melnikov, "Generalized String-Flip Model for Quantum Cluster Scattering", Department of Mathematics and Computational Physics, St.Petersburg University report, Sec.5 (1992).
[29] M.D.Kovarik, personal communication.
[30] B.R.Martin and G.C.Oades, "KN Phase Shift Analysis Including Constraints from Fixed-t Analyticity". Unpublished report of results presented at the *IVth International Conference on Baryon Resonances "Baryon 1980"* (Toronto, 14-16 July 1980); see also G.C.Oades, in *Low and Intermediate Energy Kaon-Nucleon Physics* (1981), ed. E.Ferrari and G.Violini.
[31] S.J.Watts *et al.*, Phys. Lett. 95B, 323 (1980).
[32] K.Hashimoto, Phys. Rev. C29, 1377 (1984).
[33] R.A.Arndt and L.D.Roper, Phys. Rev. D31, 2230 (1985).
[34] M.J.Corden *et al.*, Phys. Rev. D25, 720 (1982).
[35] K.Nakajima *et al.*, Phys. Lett. 112B, 80 (1982).
[36] R.E.Cutkosky, H.R.Hicks, J.Sandusky, C.C.Shih, R.L.Kelly, R.C.Miller and A.Yokosawa, Nucl. Phys. B102, 139 (1976).
[37] J.S.Hyslop, "An Analysis of K^+-Nucleon Scattering", Ph.D. thesis, Virginia Polytechnic Institute and State University (1990).
[38] S.Capstick, personal communication.
[39] N.Isgur, personal communication.
[40] R.Koniuk, personal communication.
[41] N.Isgur and G.Karl, Phys. Rev. D20, 1191 (1979).
[42] L.A.Copley, G.Karl and E.Obryk, Nucl. Phys. B13, 303 (1969).
[43] R.Koniuk and N.Isgur, Phys. Rev. D21, 1868 (1980).
[44] R.K.Carnegie *et al.*, Phys. Lett. 59B, 313 (1975).
[45] T.Barnes and G.I.Ghandour, Phys. Lett. 118B, 411 (1982).
[46] B.May *et al.*, Z. Phys. C46, 203 (1990).
[47] M.A.Kunze, Crystal Barrel Collaboration, in *Proceedings of the IVth International Conference on Hadron Spectroscopy "Hadron '91"* (College Park, Md. 12-16 August 1991), (World Scientific, 1992), pp.243-249.
[48] Obelix Collaboration, A.Adamo *et al.*, *ibid.*, pp.250-256.
[49] Particle Data Group, M.Aguilar-Benitez *et al.*, Phys. Lett. 170B, 289 (1986).
[50] Particle Data Group, K.Hikasa *et al.*, Phys. Rev. D45, VIII.58 (1992).
[51] C.J. Joachain, *Quantum Collision Theory*, (North Holland, New York, 1975).
[52] K.Maltman, personal communication.

VII. APPENDIX

The procedure we advocate for describing hadronic interactions involves simply calculating the Born order scattering amplitude for a given process using the constituent quark model. In cases where many channels contribute or one wishes to obtain nonperturbative information (such as the possible existence of hadronic bound states) then one must extract an effective potential (or effective potential matrix in the case of multichannel problems) from the Born amplitude and integrate the appropriate Schrödinger equation. The validity of this procedure and its relationship to the resonating group method are the subjects of this appendix.

Several theoretical complications arise when considering scattering of composite particles. For example, the Hamiltonian may be partitioned in many different ways corresponding to different rearrangement channels. Thus if i represents the initial channel consisting of hadrons a and b, and f represents the final channel with hadrons c and d, then we may write

$$H = H_i + V_i = H_f + V_f, \tag{91}$$

where

$$H_i = -\frac{1}{2\mu_{ab}}\nabla_R^2 + H_a + H_b \tag{92}$$

and

$$H_f = -\frac{1}{2\mu_{cd}}\nabla_R^2 + H_c + H_d. \tag{93}$$

Here $\vec{R}$ is the appropriate interhadron coordinate and μ_{ab} is the reduced mass of the constituent masses of hadrons a and b. The Hamiltonians H_a and H_b describe the hadronic wavefunctions in the initial channel. Thus we have

$$H_a\phi_{a,n}(\xi_{\mathbf{a}}) = \epsilon_{a,n}\phi_{a,n}(\xi_{\mathbf{a}}) \tag{94}$$

and similarly for the other hadrons.

In general the wavefunction must be antisymmetrized appropriately and this means summing over the various rearrangement channels with the correct weights. Thus we take the incoming wavefunction to be $\phi_a(\xi_{\mathbf{a}})\phi_b(\xi_{\mathbf{b}})\psi_0(\mathbf{R})$ where ψ_0 is a plane wave and define the antisymmetrization operator as

$$\mathcal{A} = \tfrac{1}{\sqrt{\eta}}\sum_P (-)^P P \tag{95}$$

where P is a quark exchange operator. The Born series for the process $ab \to cd$ may then be written as

$$\langle \hat{f}|t|\hat{i}\rangle = \tfrac{1}{\eta}\sum_{PP'}(-)^P(-)^{P'}\langle P\phi_c\phi_d\psi_0|\Big(V_{P'} + V_P G_c V_{P'} + V_P G_c V_c G_c V_{P'} + \dots\Big)|P'\phi_a\phi_b\psi_0\rangle. \tag{96}$$

Here G_c is the Green function in a general channel c.

The Born order expression is

$$\langle\hat{f}|T|\hat{i}\rangle = \sum_P (-)^P \langle\phi_c\phi_d\psi_0|V_i|P\phi_a\phi_b\psi_0\rangle. \tag{97}$$

This is the "prior" form of the T-matrix. The "post" form uses the potential in the final channel rather than the initial channel. The expressions are equivalent if the hadronic wavefunctions are exact and the T-matrix is evaluated on energy shell. Note that these conditions must also hold if the effective potential matrix is to be Hermitian.

Little is known about the convergence properties of the Born series. With no exchange the conditions for convergence are probably similar to those for simple potential scattering [51]. Of course exchange scattering is necessarily present when describing hadronic interactions from the quark level. At high energy there is evidence that the lowest few Born terms can be accurate [51]. However, since the potential is strong enough to cause binding in the initial and final states, the series will diverge at low energies. Nevertheless the strategy of extracting an effective potential can be useful when the Born approximation is not accurate or even when it diverges. We shall return to this point below. Despite the theoretical problems, the small nuclear binding energy, the small phase shifts seen in K^+N scattering, and the lack of quark model state mixing evidenced in most of the meson spectrum all suggest the utility of the Born approximation.

It should be stressed that the Born approximation can be useful even when the effective potential is very strong. This will be true if the Born term carries information on the dominant physics. Then the Born order scattering amplitude may be Fourier transformed to yield an effective potential which contains all of the dominant physics and may be integrated exactly. Since hadronic interactions must involve constituents, this may not be carried out in general, however it will be accurate if the new physics induced at higher order in the Born series (such as polarization effects) does not dominate at low energy. As will be discussed below, this appears to be true in many cases.

We now turn to the relationship of this approach to the resonating group method. In the following we shall restrict our attention to the single channel case. The resonating group Ansatz is then

$$\Psi = \phi_a(\xi_{\mathbf{a}})\phi_b(\xi_{\mathbf{b}})\psi(\mathbf{R}) \tag{98}$$

where ψ is an unknown function of the interhadron distance. This Ansatz must be antisymmetrized. For later convenience, we choose to separate the identity permutation. Thus the wavefunction is

$$\hat{\Psi} = \mathcal{A}\Psi = \frac{1}{\sqrt{\eta}}\left(1 + \sum_{P\neq I}(-)^P P\right)\phi_a\phi_b\psi. \tag{99}$$

Varying the Schrödinger equation with respect to ψ and rewriting the resulting expression for ψ in Lippmann-Schwinger form yields the following equation.

$$\psi(\mathbf{R}) = \psi_0(\mathbf{R}) + 2\mu_{ab}\int G_0(\mathbf{R},\mathbf{R}')V_D(\mathbf{R}')\psi(\mathbf{R}')d\mathbf{R}'$$

$$-\sum_{P\neq I}(-)^P \int G_0(\mathbf{R},\mathbf{R}')\phi_a^*(\xi_{\mathbf{a}})\phi_b^*(\xi_{\mathbf{b}})\,\left[\nabla_R^2 + k_{\rm rel}^2\right] P[\phi_a(\xi_{\mathbf{a}})\phi_b(\xi_{\mathbf{b}})\psi(\mathbf{R}')]d\xi_{\mathbf{a}}d\xi_{\mathbf{b}}d\mathbf{R}'$$

$$+ 2\mu_{ab} \sum_{P\neq I} (-)^P \int G_0(\mathbf{R},\mathbf{R}')\phi_a^*(\xi_\mathbf{a})\phi_b^*(\xi_\mathbf{b})\, V_i(\xi_\mathbf{a},\xi_\mathbf{b},\mathbf{R}')P[\phi_a(\xi_\mathbf{a})\phi_b(\xi_\mathbf{b})\psi\mathbf{R}')]d\xi_\mathbf{a}d\xi_\mathbf{b}d\mathbf{R}' \quad (100)$$

where

$$k_{\rm rel}^2 = 2\mu_{ab}(E - \epsilon_a - \epsilon_b) \quad (101)$$

and

$$V_D(\mathbf{R}) = \int \phi_a^*(\xi_\mathbf{a})\phi_b^*(\xi_\mathbf{b})V_i(\xi_\mathbf{a},\xi_\mathbf{b},\mathbf{R})\phi_a(\xi_\mathbf{a})\phi_b(\xi_\mathbf{b})d\xi_\mathbf{a}d\xi_\mathbf{b}, \quad (102)$$

and G_0 is the Green function for $\nabla_R^2 + k_{\rm rel}^2$.

The permutation operator in the third term implies that $\nabla_R^2 + k_{\rm rel}^2$ is a Hermitian operator and may be safely applied to the left. Thus the third term (the kinetic and energy exchange kernels) simplifies to

$$-\sum_{P\neq I}(-)^P \int \phi_a\phi_b P[\phi_a\phi_b\psi(\mathbf{R})]d\xi_\mathbf{a}d\xi_\mathbf{b} \equiv \int N(\mathbf{R},\tilde{\mathbf{R}})\psi(\tilde{\mathbf{R}})d\tilde{\mathbf{R}} \quad (103)$$

where $N(\mathbf{R},\tilde{\mathbf{R}})$ is the normalization kernel. Because of nontrivial permutation operators this expression is damped as $R \to \infty$ and hence it does not contribute to scattering.

We may now iterate Eq. (**??**) to see that it corresponds to the full Born series (96) with the sum over intermediate states restricted to the appropriate single channel. In particular the $R \to \infty$ limit of the first term in the series corresponds to the Born order T-matrix of Eq. (97) (for the case of elastic scattering).

Eq. (**??**) indicates that setting $V_i = 0$ in a resonating group calculation should yield a null phase shift. However if one uses approximate hadronic wavefunctions (as is almost always the case in resonating group calculations) then a residual spurious phase shift will remain. We note that Bender *et al.* [24] employ single Gaussian hadronic wavefunctions so that one expects small phase shifts upon setting $V_i = 0$. This is indeed what they found for I=0 K^+N scattering. However they obtained rather large phase shifts for the I=1 case. Since the Hamiltonian is independent of the isospin the Gaussian wavefunctions should have been equally effective in both cases and one must conclude that there is likely to be an error in the I=1 calculation. Maltman [52] has concluded that there are indeed errors in the hyperfine matrix elements in this reference.

Solving the single channel resonating group equation is similar to the process of extracting an effective potential from the Born scattering amplitude and integrating it exactly. Both methods treat the single channel subspace nonperturbatively and hence are successful when the single channel approximation is a good one. Both methods fail if (off-channel) virtual particles, polarization, wavefunction distortion, and similar effects dominate the low energy behavior of the system. As stated above, this does not seem to happen in practice. The similarity of hadron scattering amplitudes obtained from the single channel resonating group method and from integrating effective potentials has been demonstrated for several cases in Ref. [18].